1994-12-31

Characterization of Mojave Desert aerosols: Their effect on radiometer performance

Mathews, L.A.; Salgado, D.P.; Walker, P.L.

SPIE--The International Society for Optical Engineering

Conference: Society of Photo-Optical Instrumentation Engineers conference on intelligent information systems, Orlando, FL (United States), 4-8 Apr 1994; Other Information: PBD: 1994; Related Information: Is Part Of Atmospheric propagation and remote sensing 3; Flood, W.A.; Miller, W.B. [eds.]; PB: 947 p.; Proceedings/SPIE, Volume 2222

http://hdl.handle.net/10945/61037

Characterization of Mojave Desert aerosols: their effect on radiometer performance

Larry A. Mathews, Dan P. Salgado, Philip L. Walker

Larry A. Mathews, Dan P. Salgado, Philip L. Walker, "Characterization of Mojave Desert aerosols: their effect on radiometer performance," Proc. SPIE 2222, Atmospheric Propagation and Remote Sensing III, (29 June 1994); doi: 10.1117/12.178004

SPIE.

Event: SPIE's International Symposium on Optical Engineering and Photonics in Aerospace Sensing, 1994, Orlando, FL, United States

Characterization Of Mojave Desert Aerosols: Their Effect on Radiometer Performance

L.A. Mathews and D.P. Salgado
Naval Air Warfare Center, China Lake, CA
and
P.L. Walker
Department of Physics
Naval Postgraduate School, Monterey, CA

ABSTRACT

The Visibility Impact Summer Study held from July to September 1990 was an intense, comprehensive study intended to measure aerosol size and chemical composition and to ascertain their optical effects. Size distributions for particle diameters from 0.01 to 10 μ were measured at hourly intervals and particle samplers were used to obtain chemical compositions at daily intervals at Tehachapi Pass and Edwards AFB, California. The extracted aerosol characteristics are discussed and compared to the desert aerosol model in LOWTRAN and the size and estimated composition of aerosols at China Lake reported upon earlier. We obtain relationships between aerosol mass and wind speed, diurnal size changes, and meteorological effects. Secondarily, extinction was calculated and used with LOWTRAN and radiosonde data for examination of aerosol effects on narrow band 3-5 and 8-12 μ imaging radiometer performance.

1. INTRODUCTION

Objectives of the present work are to add to the data base of the characteristics of desert aerosols and to examine further[1] their effect on imaging radiometer performance. Simultaneous visibility and meteorological data and aerosol filter samples were taken at four wide-spread locations in the western Mojave Desert of California. Locations of the sampling sites are shown in the first figure. In addition, aerosol size distribution measurements were made at two of these locations in the vicinity of the Antelope Valley, California. Sampling started the first week in July and ran through the second week in September 1990. Data were taken twenty-four hours a day in most cases and from 0700 to 1200 and 1200 to 1700 PDT where it was desired to obtain diurnal aerosol composition. Only the Edwards AFB site will be discussed in this article.

The Antelope Valley is part of the southwestern Mojave Desert lying fifty miles north of Los Angeles International Airport. The Antelope Valley is separated from the Los Angeles and San Fernando Valley air basins by the San Gabriel Mountains. The Tehachapi Mountains, to the west, separate the Antelope Valley from the San Joaquin Valley. Combustion aerosols are transported from the San Joaquin Valley through the Tehachapi Pass and through the Soledad and Cajun passes from the Los Angeles air basin. Thus the valley's atmosphere contains a spatially and temporally complex mixture of aerosols of urban, industrial and desert origin.

2. EXPERIMENTAL PROCEDURE

2.1 Meteorological Data

Radiosonde data were taken daily at 0230 PST at Edwards and at 0530 at China Lake at 1000 foot intervals from surface to 100,000 feet. Wind speed and direction were obtained at China Lake and Edwards with Handar Wind Speed and Direction Sensors while temperature and dew point were obtained with a Handar Temp/RH Probe. Climtronics instruments were used to take similar data at Telhill and Tehachapi. The meteorological instruments were placed ten meters above the ground and recorded data 24 hours a day.

2.2 Particle Sizers

Particle sizers were located at Edwards and Tehachapi. The sizers were mounted four meters above the ground and took hourly data twenty-four hours a day. At Edwards aerosol size distributions were obtained with a TSI Differential Mobility Particle Sizer (DMPS) for particles with diameters in the range 0.01 to 0.8 μ and with an APS-33 Aerosol Particle Sizer for particle diameters ranging from 0.5 to 30 μ. Aerosol size distribution measurements were also taken at Tehachapi with a TSI Electrical Aerosol Analyzer (EAA) for particles in the size range 0.01 to 0.6μ and a Laser Aerosol Spectrometer (LAS-X model) Optical Particle Counter for particles in the size range 0.09 to 3 μ. The size range of the Tehachapi instruments is too small for dust; thus, the data from Edwards will be emphasized in this article.

2.3 Aerosol Filter Samplers

0-8194-1526-X/94/$6.00

The continuous samples were taken with Wedding 2X4 Filter Samplers. These samplers acquired one total and three fine aerosol samples daily. The total filter sample and two of the fine filter samples were collected on Teflon filters for mass, absorption, and elemental composition. The second fine Teflon filter serves as a data quality check. The third fine particle filter is composed of quartz and is used for elemental and organic carbon determination.

PM2.5 and PM10 aerosol filter samplers mounted three meters above the ground were operated continuously at all of the sites. In addition, two five hour samples were taken daily from 0700 to 1200 and from 1200 to 1700 PDT at Edwards and Tehachapi. The five hour aerosol samples were made with NEA Sequential Filter Samplers (SFS). The sequential filter sampler allows air to be drawn through a size-selective inlet and through two different sets of filter media. Solenoid valves are controlled by a timer switch with up to six sets of filters at pre-set intervals. A vacuum pump draws air through these filters when the valves are open. The PM10 size fraction is transmitted through a Sierra-Andersen 254I size-selective inlet into a plenum. The PM2.5 fraction is transmitted through a Bendix 240 cyclone into a separate sampling unit. A timer is set to cycle sequentially between six sets of filters. Two sets of samples were collected every day from at 1200 and 1700 PDT. Two sets of filters sampled simultaneously in both PM10 and PM2.5 SFS. One set consists of a Teflon-membrane filter which collects particles for gravimetric and x-ray fluorescence (XRF) analyses. The other fine filter holder consists of a quartz-fiber filter. Deposits on this filter are submitted to ion and carbon analyses.

Chlorine, nitrate, sulfate, ammonium ions and potassium masses were determined gravimetrically as each was chemically extracted from the Teflon filter. XRF analysis was performed on Teflon-membrane filters. Analyses were performed using a Kevex Corporation Model 700/8000 energy dispersive x-ray (EDX) fluorescence analyzer. The analyses were controlled, spectra acquired, and elemental concentrations calculated by software implemented on an LIS 11/23 microcomputer interfaced to the analyzer.

3.0 AEROSOL ANALYSIS

3.1 Composition

Only the composition of aerosols captured on the NEA SFS five-hour diurnal filter samplers located at Edwards will be discussed in this report. The average composition of the aerosols captured on these filters is tabulated in Table 1. The PM10 filter captured all particles smaller than ten microns; whereas, the PM2.5 filters were used to capture particles smaller than 2.5 microns diameter. The quartz fiber filter was used to capture organic carbon for analysis. The anomalously high organic content of accumulation mode aerosols in the western Mojave has been observed several times before and there has been some fear that this is due to contamination. Therefore, filters were randomly examined for organic carbon contamination before they were used in the field. Blank quartz-fiber filters were heated for at least three hours at 900 °C before use and kept refrigerated prior to heating.

Since the ammonium ion mass was not measured it has to be estimated by assuming that the nitrate is present as ammonium nitrate, NH_4NO_3, and sulfate present as ammonium sulfate $(NH_4)_2SO_4$. (Atmospheric sulfate can also be present as sulfuric acid if insufficient quantities of ammonium are not available to neutralize it.) If the sulfate neutralization assumption is valid then ammonia add 5.3% to the total fine particle mass, so that ammonium nitrate becomes 5.8% and ammonium sulfate 19.8%. The relative number of moles of sulfur in excess to the total of the PM2.5 sulfur listed in the lower part of the table approximates the number of moles of calcium. This near molar equality is also true in the PM10 column. Probably, the sulfur and calcium are combined as gypsum, $CaSO_4$ so that 21% of the PM10 aerosol mass would be gypsum.

The lower part of Table 1 is a comparison of the elemental composition of the PM10 aerosol with the composition of clays. The best match is with illite clay, which is common to deserts. (The compositions of the listed clays are averages obtained from an extensive review of the literature in Ref. 2; thus, compositional agreement cannot be expected to be exact.) The PM10 aerosol is 80% illite clay by mass, exclusive of the PM2.5 aerosols tabulated in the upper part of the table.

3.2 Wind Speed Dependence of Aerosol Mass

Wind Speed dependence of the mass (in $\mu g/m^3$) of PM10 aerosols in Figure 2 was obtained by plotting five hour integrated mass captured on the NEA Sequential Filter Sampler with wind speeds averaged for the same five hours. The NEA samplers were operated from 0700 to 1200 and again, with new filters, from 1200 to 1700 PDT. The U-shaped dashed line in the figure is a least-squares fit to the data. A more sensible fit would be no Wind Speed dependence below 6 m/sec and an exponential fit that approximates the least-squares curve for greater wind speeds. This fit is indicated by the solid lines in the figure. Thus, the "instantaneous" Wind Speed dependence of dust mode mass is given by Equation 1.

$$m = \begin{cases} 20\exp(0.23u) \ (\mu g/m^3) & \text{for } u > 6 \text{ m/sec} \\ 20 & \text{for } u < 6 \text{ m/sec} \end{cases} \quad (1)$$

More commonly, it is assumed that small particle aerosol mass depends upon 24 hour averaged Wind Speed. This is plotted in Figure 3 with the averaging period ending at the end of a five hour NEA SFS sample period. The U-shaped dashed curve is again a least-squares fit. A linear regression fit to the semi-log data yields an exponential relationship to aerosol mass and wind speed given by Equation 2.

$$m = 11.9\exp(0.17u) \quad (2)$$

Short time wind speed averaging clearly yields a better fit to the data.

Aerosol mass in the size range .06 to 1 μ diameter is dominated by accumulation mode particles typically made of the materials listed in the upper part of Table 1. Aerosols in the size range 1 to 10 μ are typically clays. There is yet another size distribution mode due to blowing sand, which is supposed to be made of quartz. Therefore, the composition of the PM10 captured particles might also be wind speed dependent. Figure 4 is a plot of the ratio of PM10 silicon to aluminum versus the short-term averaged wind speed. Clearly, even a part of a silicon dominated sand mode is not being captured even at wind speeds of 9 m/sec.

3.3 Size Distribution

An objective of this report is to model the effect of aerosols on imaging radiometer performance. Radiometer performance in ambient conditions was reported upon previously.[1] The present data set contains aerosol size distribution data at wind speeds of up to ten meters per second. Therefore, only radiometer performance in these conditions need to be looked at. Unfortunately, the size distribution characterization is incomplete because only the APS33 was operating on the day that the higher than normal wind speeds occurred. However, accumulation mode aerosols do not significantly contribute to extinction for wave lengths greater than two microns; whereas, the infrared imaging radiometers considered operate at greater wavelengths. Wind speed history for 25 August 1990 is plotted up in Figure 5.

The size distributions of Figure 6 are for pre-storm winds at 0200, maximum aerosol loading at 1600 with wind speed at 8.9 m/sec, and post-storm at 2400. Aerosol mass is plotted in Figure 7. Both size distributions were calculated from aerodynamic particle data assuming particle specific gravity of 2.7. The pre-storm aerosol environment was dominated by accumulation mode particles with light dust loading. The post-storm atmosphere is dominated by residual dust with no apparent accumulation mode particles. Maximum particulate loading at wind speeds near 10 m/sec is dominated by dust mode clay particles with the possible presence of a larger mode with mode diameter of about seven microns.

3.4 Dust Optical Characteristics

Optical characteristics of the dust were calculated using the EOSAEL Mie Scattering code[3] and infrared indices of refraction of illite clay from Ref. 4. The authors were not able to obtain indices of refraction for gypsum in time for this report. Also, the formula for illite clay in the Querry report is given by $(K,H_3O)Al_2[(OH)_2/ALSi_3O_{10}]$, which contains no iron. Those optical characteristics needed for input to LOWTRAN[7] are in Figures 8 and 9. These figures are preliminary due to the absence of the effect of iron and gypsum's index of refraction in the Mie calculations.

4. RADIOMETER PERFORMANCE

A recalculation of imaging radiometer performance using the new aerosol data was performed in exactly the same as it was in Ref. 1. The results of the recalculation are in Table 2. Use of the eight to twelve micron range is even more advantageous during dust storms as long as there is no blowing sand. Contrast transmittance of the MagnavoxTCIR approximately doubles in the seven to nine micron transmission window.

5. DISCUSSION

Results from the present study differ in several significant ways from that of Longtin, et al[5]. First, the accumulation (or water soluble) mode ispredominantlyy organic carbon instead of being composed of sulfates. That may be due to the proximity to large urban,

industrial and oil producing and refining regions. Secondly, the Longtin model does not even include the dust mode, which is the predominant continental large aerosol mode. It may be that the Sahara Desert from which part of their model is extracted[6] has been depleted of small particle clays. Last, there is a hint in the current study of the presence of the so called blowing sand mode whichh is supposed to appear when wind speeds exceed 10 m/sec. However, the composition of this mode is that of clay, not sand.

6. REFERENCES

1. Walker, P.L., Mathews, L.A., "The Effect of Smog and Dust on the Relative Performance of Mid and Far Infrared Detectors", SPIE Proc. 1968, Orlando, FL, April 1993.
2. Weaver, C.E. and Pollard, L.D., The Chemistry of Clay Minerals, Elsevier, New York, 1973.
3. Duncan, L.D., ed., "EOSAEL 80 Volume I: Technical Documentation", U.S. Army Atmospheric SciencesLaboratory, White Sands Missile Range, NM ASL, January 1981. 271 pp.
4. Querry, M.R., "Optical Constants", U.S. Army Chemical Research, Development andEngineering Center, Aberdeen Proving Ground, Maryland, June 1985. 413 pp. AD A158623.
5. Longtin, D.L., Shettle, E.P., Hummel, J.R., and Pryce, J.D., "A Desert Aerosol Model forRadiative Transfer Studies", in Aerosols and Climate, Hobbs, P.V. and McCormick, M.P., eds., Deepak Publishing. 1988.
6. d'Almeida, G.A., "On the variability of desert aerosol radiative characteristics", J. Geophys. Res. 92 D33017 (March 20, 1987).
7. F.X. Kneizys, E.P. Shettle, W.O. Gallery, J.H.V Chetwynd, Jr., L.W. Abreu, J.E.A. Selby, S.A. Clough, and G.P. Anderson, "Atmospheric Transmittance/Radiance: Computer Code LOWTRAN7", Air Force Geophysics Laboratory, Hanscom AFB, Mass. 01731, August 1988. 146 pp. AFGL-TR-88-0177.

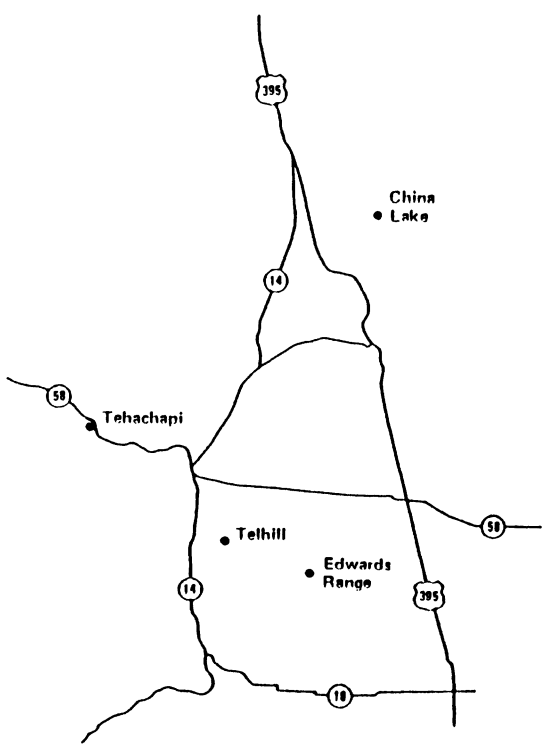

Figure 1. Road Map Locating Measurement Sites if Mojave Desert.

0-8194-1526-X/94/$6.00

Table 1. Composition of Aerosol Captured on PM2.5 and PM10 Filters. Comparison of the PM10 aerosol with clay compositions indicates that Edwards dust is composed of illite clay and gypsum. The accumulation mode aerosols, however, are predominantly organic.

Ions	% Mass		% Mass of Clay Elements									
	PM2.5	PM10	Illite	Glauconite	Montmorillinte	Chlorite	Illite Montmorillinite	Chlorite Montmorillinite	Palygorskite	Sepiolite	Kaolinite	Allophanes
Chloride	0.4											
Nitrate	5.0											
Sulfate	16.4											
Ammonium												
Organic Carbon	42											
Elemental Carbon	7.4											
Elements												
Al	4.0	20.4	24	9.15	21.93	33.52	28.5	12.1	6.82	0.6	35.18	44.95
Si	10.4	47.9	51.7	49.22	59.49	39.85	51.5	41.2	61.6	52.5	48.8	26.68
P		0.04										10.57
S	6.9	5.6										0.22
Cl		0.07										
K	2.3	7.1	5.59	6.88	0.34	1.61	9.07	0.22			0.4	
Ca	1.9	6.3	0.97	0.64	1.18	0.15	0.05	1.4	0.67	0.47	0.22	2.37
Ti	0.3	0.9	0.68		0.25	1.03	0.77	0.04			0.61	
Mn	0.1	0.2										
Fe	3.5	11	4.57	21.38	3.97	4.56	1.52	2.13	0.87	3.6	1.24	0.12

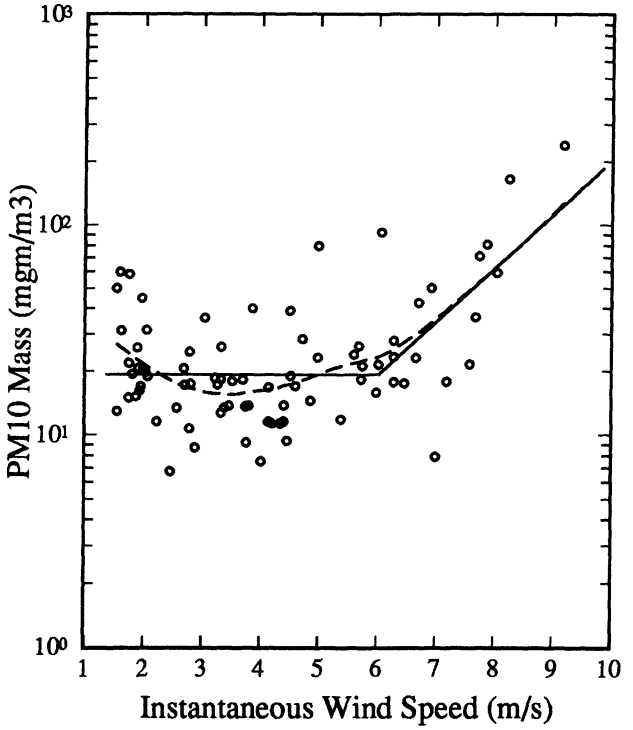

Figure 2. SFS Filter Mass vs Five Hour Averaged Wind Speed.

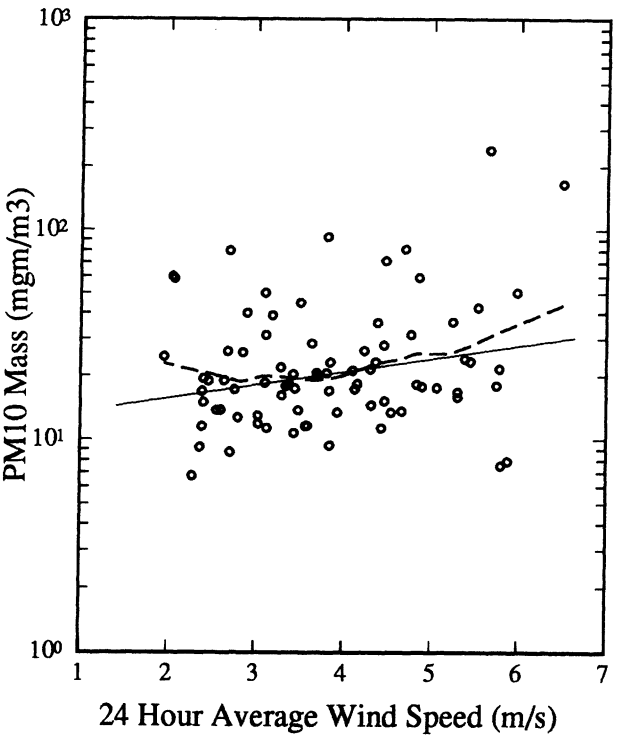

Figure 3. SFS Filter Mass vs 24 Hour Averaged Wind Speed.

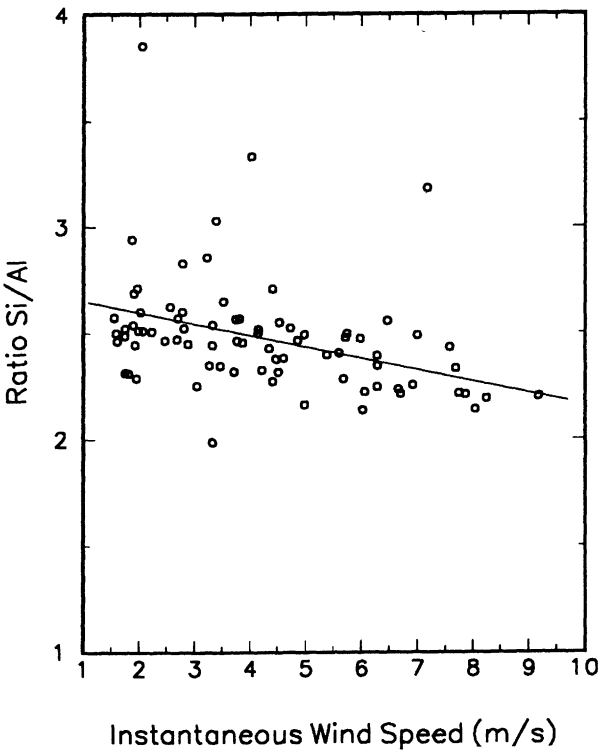

Figure 4. Silicon to Aluminum Mass Ratio vs Wind Speed. The authors do not know why ratio decreases.

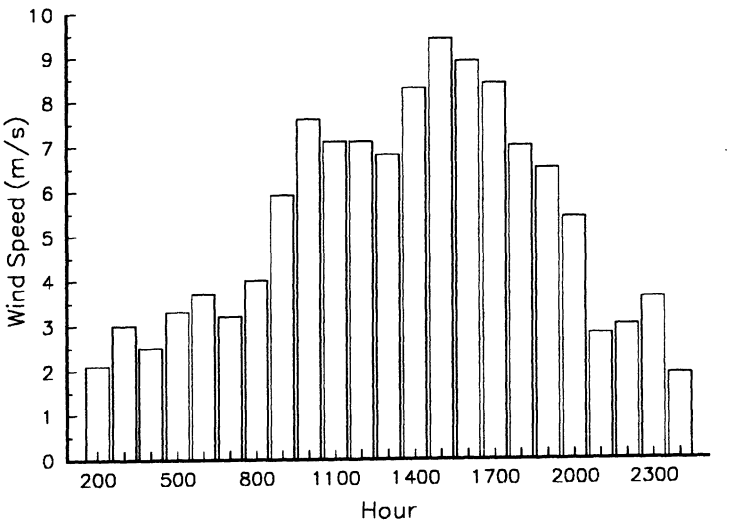

Figure 5. Wind Speed History of 25 August 1990.

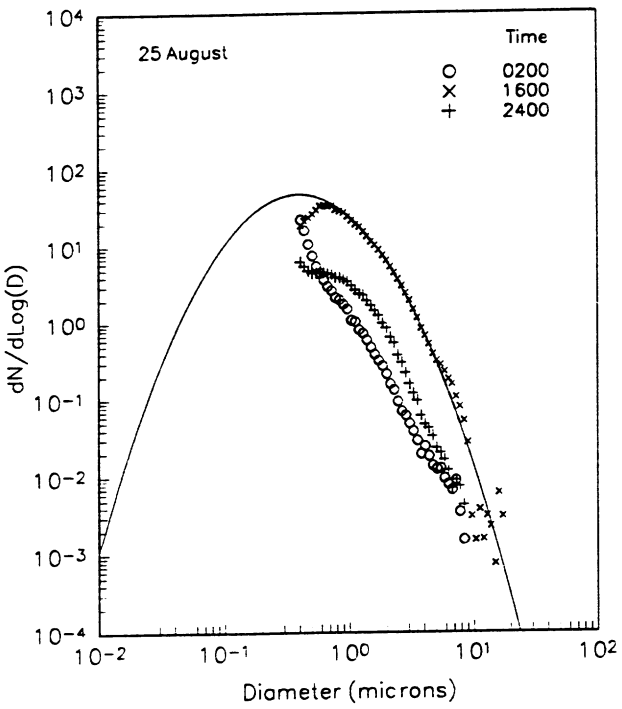

Figure 6. Number Distribution for During Peak Mass Loading of 25 August.

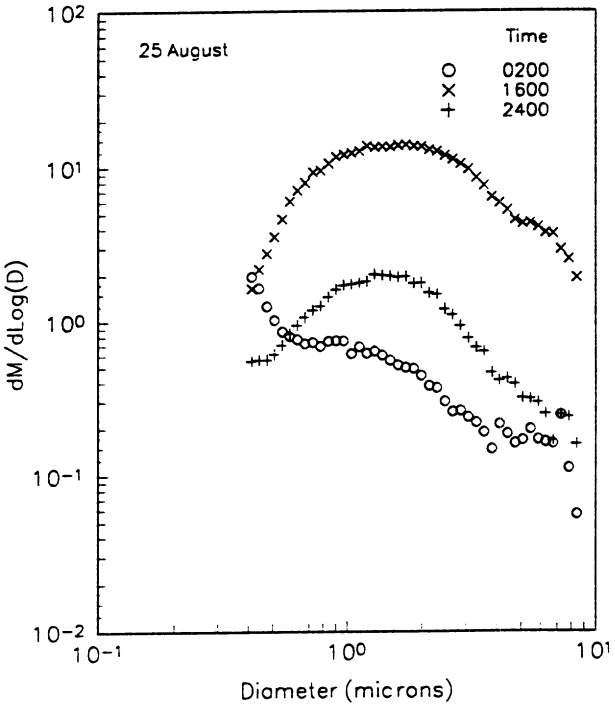

Figure 7. Mass Distribution at Time of Peak Mass Loading.

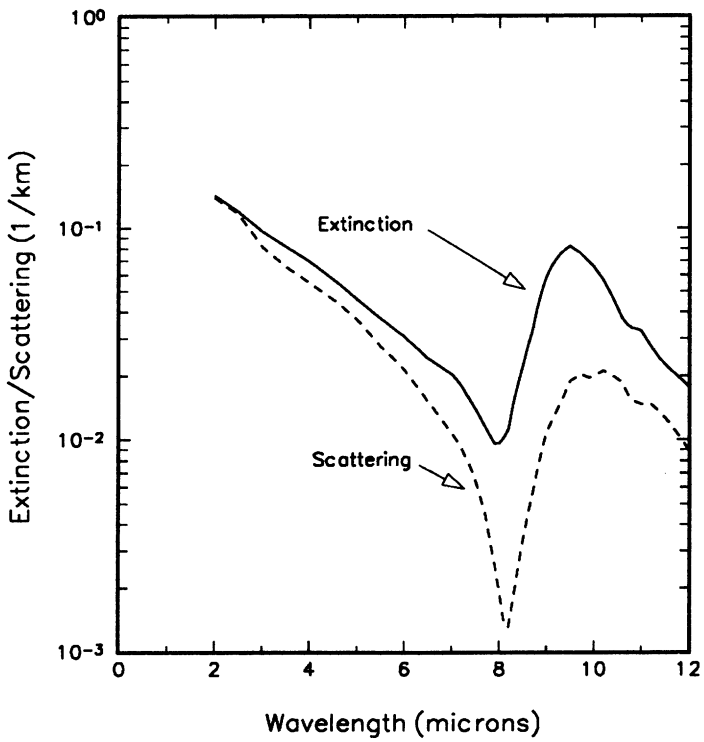

Figure 8. Extinction and Scattering Coefficeints of Aerosol at Time of Peak Mass Loading.

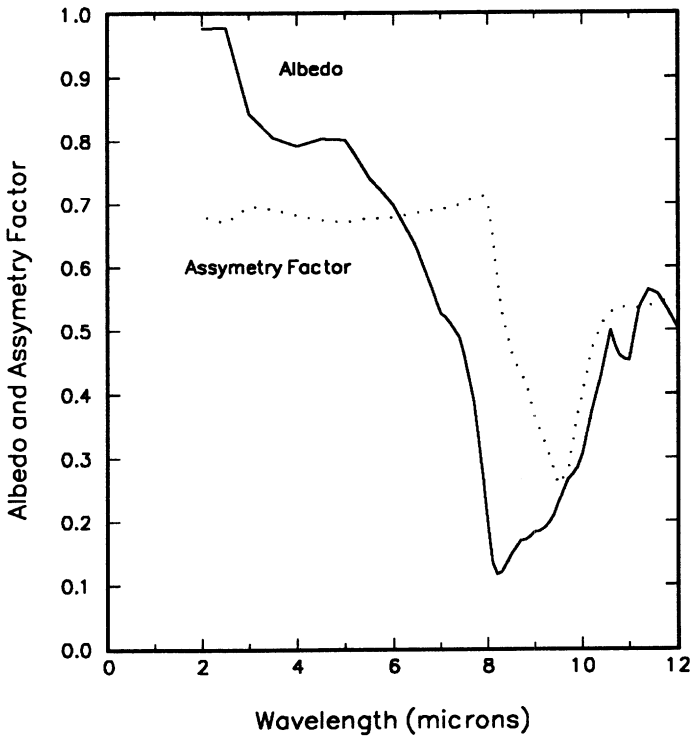

Figure 9. Assymetry Factor and Albedo During Peak Mass Loading.

Table 2. Imaging Radiometer Contrasts for the wind storm dust using Subarctic Atmospheric model in LOWTRAN 7. Visibility is 63.4 km and range to background is 30 km. The background is assumed to be a blackbody at 259.29 °K.

Mid Infrared		Far Infrared	
Imager Name	Contrast	Imager Name	Contrast
MagnavoxTCIR	.00125	MagnavoxTCIR	.0146
AGA 680	.00090	Inframetrics 610	.0164
AGA 750	.00	Barr & Stroud IR18	.0115
Inframetrics 525	.0007	Inframetrics 2100	.0145
Agema 880	.0009	AGA 661	.0146
Filtered Agema 880	.0006		
AGA 661	.00		